Dynamic Soaring in Hurricanes

Joachim Grenestedt
Mechanical Engineering and Mechanics
Lehigh University
Bethlehem, Pennsylvania

Corey Montella and John Spletzer
Computer Science and Engineering
Lehigh University
Bethlehem, Pennsylvania

***Abstract*—The potential for a gliding UAV to sustain flight by dynamically soaring in a hurricane is investigated. Leveraging extensive storm observations, the wind profile of the hurricane eye is modeled as a continuous function that is zero at the center and increases as a power of the radius. We then derive the equations of motion for a UAV flying in this wind field, and prove analytically that if the wind field exponent $n = 1$, dynamic soaring is not possible. This analytical result is also validated in simulation. We also provide extensive simulation results for the case where the wind field exponent $n > 1$. These results indicate that dynamic soaring is in fact possible for such storms, and the velocity gain for a single dynamic soaring cycle is correlated with the wind field gradient.**

I. Introduction & Related Work

In this paper, we investigate the potential for a gliding UAV to dynamically soar in the radial wind gradients associated with a tropical cyclone, *i.e.*, a hurricane. Dynamic soaring (DS) is a technique whereby horizontal wind that varies in strength or direction is used to support flight. Rayleigh is usually credited for first suggesting that soaring could be accomplished in a horizontal but non-uniform wind field [1]. Seabirds like the albatross are known to travel hundreds of kilometers in a single day utilizing dynamic soaring [2]. Save for an anecdotal flight in Australia in 1974, attempts for sustained dynamic soaring of manned gliders do not appear to have been fully successful at this time. However, radio controlled hobby aircraft routinely dynamically soar in the steep wind gradients on the leeward side of mountain ridges, and have reached speeds over 600 km/hr [3].

In the traditional DS paradigm, the wind gradient is in the vertical direction and wind speeds increase with altitude (although this need not be the case). The general soaring strategy for such a wind field is for the aircraft to climb into the wind gradient in order to gain altitude as well as airspeed (or at least not lose too much airspeed), and then dive with the wind to gain airspeed. Under appropriate conditions, the energy gained from such a trajectory can support perpetual flight. A number of papers have been devoted to optimizing trajectories of dynamically soaring aircraft, flying either in near-ground wind gradients or in wind gradients associated with high altitude jet streams. These include the works of Boslough [4], Zhao [5], Sachs and da Costa [6], Gordon [7], Akhtar *et al.* [8], and Lawrance and Sukkarieh [9]. Deittert *et al.* looked at the dynamic soaring problem using differential flatness to transform the optimization problem [10]. Our own work in this area includes [11] and [12], where we investigated trajectory generation for supporting perpetual flight in the jet stream by dynamic soaring.

These previous results lead us to investigate the potential for a gliding UAV to achieve *sustained* dynamic soaring in the radial wind field associated with a hurricane. If achievable, this could enable long-term, automated, in-situ storm monitoring. On the surface, the answer to the hurricane soaring question would appear to be straightforward: By flying away from the hurricane eye (heading into the wind), turning downwind, and flying back towards the eye, we would mimic the traditional DS paradigm for vertical wind gradients. As we shall see, the correct answer to this question is significantly more complicated. Through both analytical and numerical results, we show that for one standard hurricane wind model, dynamic soaring is impossible using radial wind gradients alone. However, we also provide numerical results that indicate DS may be achievable for alternate wind profiles with this same model. To our knowledge, these are the first results reporting on exploiting hurricane wind fields for sustained dynamic soaring of UAVs.

II. Hurricane Model

Hurricanes are a class of tropical cyclone that originate in the Atlantic or Eastern Pacific oceans. In the northern hemisphere, where hurricanes form, strong winds cycle counter-clockwise around a structure known as the hurricane eye, a typically circular, low pressure region of relatively calm winds. The diameters of hurricane eyes vary from as small as 3 km [13] to as large as 370 km [14], with an average diameter of around 45 km [15]. Winds at the center of the eye are typically still, and increase radially to a maximum windspeed at the hurricane eyewall. Hurricanes are ranked and classified by maximum sustained wind speed, which varies from 33 m/s to 70 m/s [16].

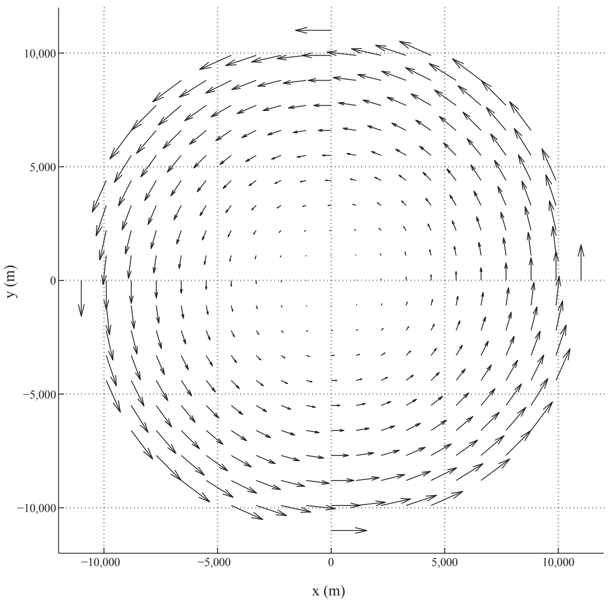

Fig. 1. Example hurricane wind field. In this instance, $W_{max} = 64m/s$, $R_{max} = 11000m$, and $n = 2$.

The wind within the eye was modeled as a parametric vortex as suggested by Willoughby *et al.* [17]:

$$W_x = -W_{max}\left(\frac{r}{R_{max}}\right)^n \sin\theta \tag{1}$$

$$W_y = W_{max}\left(\frac{r}{R_{max}}\right)^n \cos\theta \tag{2}$$

$$r = \sqrt{x^2 + y^2}$$

$$\tan\theta = \frac{y}{x}$$

where, W_{max} is the maximum tangential wind velocity, R_{max} is the radius where the maximum wind is encountered, n is the wind field exponent, x and y are Cartesian coordinates, and r and θ are polar coordinates in the hurricane wind field. A visualization of this model is depicted in Figure 1 for $n = 2$. Note that the generalized time derivative of the wind is the total derivative as seen by the aircraft, i.e.

$$\dot{W}_i = \sum_{j=1}^{3} \frac{\partial W_i}{\partial x_j}\dot{x}_j + \frac{\partial W_x}{\partial t}$$

For our analysis, we assume $\frac{\partial W_x}{\partial t}$ is zero. In a first approximation of a hurricane eye it will be assumed that the vertical wind is negligible ($W_z = 0$), and that the other wind components only depend on in-plane coordinates x and y; thus

$$\dot{W}_x = \frac{\partial W_x}{\partial x}\dot{x} + \frac{\partial W_x}{\partial y}\dot{y}$$

$$\dot{W}_y = \frac{\partial W_y}{\partial x}\dot{x} + \frac{\partial W_y}{\partial y}\dot{y}$$

III. Aircraft Equations of Motion

Let the UAV track relative to the air be

$$\mathbf{e}_x^v = \cos\gamma\sin\psi\mathbf{e}_x + \cos\gamma\cos\psi\mathbf{e}_y + \sin\gamma\mathbf{e}_z \tag{3}$$

where ψ is the aircraft heading angle measured clockwise from North, γ is air-relative flight path angle, and $\mathbf{e}_i$ is a unit vector parallel to the Cartesian reference (inertia) frames; $\mathbf{e}_x$ points East, $\mathbf{e}_y$ North, and $\mathbf{e}_z$ up. When there is no roll

$$\mathbf{e}_y^v = \cos\psi\mathbf{e}_x - \sin\psi\mathbf{e}_y \tag{4}$$

$$\mathbf{e}_z^v = \sin\gamma\sin\psi\mathbf{e}_x + \sin\gamma\cos\psi\mathbf{e}_y - \cos\gamma\mathbf{e}_z \tag{5}$$

The flight trajectory follows the air relative track plus the wind drift

$$\begin{aligned}\dot{\mathbf{r}} &= \dot{x}\mathbf{e}_x + \dot{y}\mathbf{e}_y + \dot{z}\mathbf{e}_z\\ &= V\mathbf{e}^v + \mathbf{W}\\ &= (V\cos\gamma\sin\psi + W_x)\mathbf{e}_x +\\ &\quad (V\cos\gamma\cos\psi + W_y)\mathbf{e}_y +\\ &\quad (V\sin\gamma + W_z)\mathbf{e}_z\end{aligned}$$

where x, y, and z are Cartesian coordinates, V is airspeed, and a dot represents a time derivative.

As previously mentioned, in a first approximation of a hurricane eye it will be assumed that the vertical wind is negligible ($W_z = 0$), and that the other wind components only depend on in-plane coordinates x and y; thus

$$\begin{aligned}\dot{\mathbf{r}} =&(V\cos\gamma\sin\psi + W_x)\mathbf{e}_x +\\ &(V\cos\gamma\cos\psi + W_y)\mathbf{e}_y +\\ &V\sin\gamma\mathbf{e}_z\end{aligned} \tag{6}$$

The drag D on the aircraft is in the direction of $-\mathbf{e}_x$, and the lift L on the aircraft is in the direction of $\mathbf{e}_z$. Thus the forces acting on the aircraft are

$$\mathbf{F} = -D\mathbf{e}_x + (L - mg)\mathbf{e}_z \tag{7}$$

We can then equate the derivative of eq. (6) to eq. (7) by Newton's second law

$$\begin{aligned}\mathbf{F} =&m\ddot{\mathbf{r}}\\ =&m(\dot{V}\cos\gamma\sin\psi - V\sin\gamma\sin\psi\dot{\gamma}+\\ &V\cos\gamma\cos\psi\dot{\psi} + \dot{W}_x)\mathbf{e}_x+\\ &m(\dot{V}\cos\gamma\cos\psi - V\sin\gamma\cos\psi\dot{\gamma}-\\ &V\cos\gamma\sin\psi\dot{\psi} + \dot{W}_y)\mathbf{e}_y+\\ &m(\dot{V}\sin\gamma + V\cos\gamma\dot{\gamma})\mathbf{e}_z\\ =&-D\mathbf{e}_x + (L - mg)\mathbf{e}_z\\ =&(-Dcos\gamma\sin\psi - L\cos\mu\sin\gamma\sin\psi+\\ &L\sin\mu\cos\psi)\mathbf{e}_x+\\ &(-D\cos\gamma\cos\psi - Lcos\mu\sin\gamma\cos\psi-\\ &L\sin\mu\sin\psi)\mathbf{e}_y+\\ &(-D\sin\gamma + L\cos\mu\cos\gamma - mg)\mathbf{e}_z\end{aligned}$$

Scalar multiplication with eqs. (3) to (5) respectively leads to the full set of equations of motion

$$\dot{x} = V\cos\gamma\sin\psi + W_x \tag{8}$$

$$\dot{y} = V\cos\gamma\cos\psi + W_y \tag{9}$$

$$\dot{z} = V\sin\gamma \tag{10}$$

$$\begin{aligned}m\dot{V} =& -D - mg\sin\gamma-\\ &m\cos\gamma\left(\dot{W}_x\sin\psi + \dot{W}_y\cos\psi\right)\end{aligned} \tag{11}$$

$$\begin{aligned}mV\cos\gamma\dot{\psi} =& L\sin\mu - m\dot{W}_x\cos\psi+\\ &m\dot{W}_y\sin\psi\end{aligned} \tag{12}$$

$$\begin{aligned}mV\dot{\gamma} =& -L\cos\mu - mg\cos\gamma+\\ &m\sin\gamma\left(\dot{W}_x\sin\psi + \dot{W}_y\cos\psi\right)\end{aligned} \tag{13}$$

where V is the UAV airspeed, m is its mass, D is the drag force, L is the lift force, μ is the roll, and g is the acceleration due to gravity.

IV. Analytical Results For $n = 1$

For our analysis, we used Hurricane Charley as our archetype storm. According to [18], maximum wind speeds at landfall for Charley were 125 knots (64.3 m/s). More importantly, the high winds were constrained to a relatively small footprint of 6 nautical miles from the center (11 km). This combination of high W_{max} and low R_{max} provides wind gradients that, from our experience, could support more traditional forms of dynamic soaring.

Observations from 493 storm profiles in [17] indicate that a wind field exponent of $n = 1$ (*i.e.*, wind velocities increasing linearly with radius) would be appropriate for such a hurricane. With this motivation, we now prove that for an aircraft soaring in three dimensions, including gravity, but neglecting drag, dynamic soaring in a hurricane with wind field exponent $n = 1$ is not possible by exploiting radial wind gradients alone.

First we simplify eqs. (1) and (2) for a hurricane with wind field exponent $n = 1$

$$\begin{aligned}W_x &= -W_{max}\frac{r}{R_{max}}\sin\theta = -\frac{W_{max}y}{R_{max}}\\ W_y &= W_{max}\frac{r}{R_{max}}\cos\theta = \frac{W_{max}x}{R_{max}}\\ \frac{\partial W_x}{\partial x} &= 0\\ \frac{\partial W_x}{\partial y} &= -\frac{W_{max}}{R_{max}}\\ \frac{\partial W_y}{\partial x} &= \frac{W_{max}}{R_{max}}\\ \frac{\partial W_y}{\partial y} &= 0\end{aligned}$$

The equations of motion are as in eqs. (8) to (10). For $n = 1$, equation (11) becomes

$$\begin{aligned}\dot{V} &= -\cos\gamma\sin\psi\dot{W}_x - \cos\gamma\cos\psi\dot{W}_y - g\sin\gamma\\ &= -\frac{\dot{x} - W_x}{V}\dot{W}_x - \frac{\dot{y} - W_y}{V}\dot{W}_y - g\frac{\dot{z}}{V}\\ &= \frac{\dot{x} - W_x}{V}\frac{W_{max}}{R_{max}}\dot{y} - \frac{\dot{y} - W_y}{V}\frac{W_{max}}{R_{max}}\dot{x} - g\frac{\dot{z}}{V}\\ &= \frac{W_{max}}{VR_{max}}\left(W_y\dot{x} - W_x\dot{y}\right) - g\frac{\dot{z}}{V}\end{aligned}$$

The time derivative of the air-relative kinetic energy is

$$\dot{E} = mV\dot{V} = \frac{mW_{max}}{R_{max}}\left(W_y\dot{x} - W_x\dot{y}\right) \tag{14}$$

We find the total change in energy of a DS cycle by integrating (14) over a closed loop

$$\int_{t_0}^{t_1} \dot{E}dt = \int_{t_0}^{t_1} \Big(\frac{mW_{max}}{R_{max}} W_y \dot{x} - \frac{mW_{max}}{R_{max}} W_x \dot{y} - mg\dot{z} \Big) dt$$
$$= \oint \Big(\frac{mW_{max}}{R_{max}} W_y dx - \frac{mW_{max}}{R_{max}} W_x dy - mgdz \Big)$$

by applying Stokes' Theorem, we arrive at

$$= \iint \left\{ \left(\frac{\partial(-mg)}{\partial y} + \frac{mW_{max}}{R_{max}} \frac{\partial W_x}{\partial z} \right) dydz + \left(\frac{\partial(mg)}{\partial x} + \frac{mW_{max}}{R_{max}} \frac{\partial W_y}{\partial z} \right) dxdz - \frac{mW_{max}}{R_{max}} \left(\frac{\partial W_x}{\partial x} + \frac{\partial W_y}{\partial y} \right) dxdy \right\} = 0$$

This result indicates that for a wind profile of $n = 1$, dynamic soaring of a UAV in a hurricane is not possible. Note also that by neglecting drag, we are presenting the best possible case for an aircraft. Energy will be lost in practice.

V. TRAJECTORY OPTIMIZATION

To this point, we have analytically shown that dynamic soaring in a wind field with exponent n=1 is not feasible. However, in practice wind profiles can vary dramatically from storm to storm and over time. For example, in [17] hurricane instances with similar wind speeds to our archetype and wind profiles fitting $n \approx 2.5$ and higher were also observed. As our analytical results to this point are limited to n=1, we decided to investigate alternate wind field exponents using a non-linear optimization approach. Previously we showed that a feasible dynamic soaring trajectory can be modeled through non-linear constraints on the aircraft state and control inputs [12]. We model the hurricane soaring problem similarly.

The equations of motion that need to be solved are eqs. (8) to (10) and eqs. (11) to (13), rewritten as eqs. (15) to (17)

$$\dot{V} = -\cos\gamma \left(\sin\gamma \dot{W}_x + \cos\psi \dot{W}_y \right) - g\sin\gamma \tag{15}$$

$$\dot{\psi} = \frac{\frac{L}{m}\sin\mu + \sin\psi \dot{W}_y - \cos\psi \dot{W}_x}{V\cos\gamma} \tag{16}$$

$$\dot{\gamma} = \frac{L}{Vm}\cos\mu - \frac{1}{V} g\cos\gamma + \frac{1}{V}\sin\gamma \left(\sin\psi \dot{W}_x + \cos\psi \dot{W}_y \right) \tag{17}$$

where L is assumed to be

$$L = C_L S_w \frac{\rho V^2}{2}$$

where C_L is the coefficient of lift, S_w is the wing planform area, and ρ is the air density. If t_f is the total time for one complete dynamic soaring cycle, then the optimization problem can be formulated as

$$\max \quad V(t_f) - V(0)$$

subject to the initial conditions

$$\gamma(0) = 0$$

the constraints

$$0 \le r \le R_0$$
$$|\dot{\psi}| \le \dot{\psi}^{max}$$
$$|\dot{\mu}| \le \dot{\mu}^{max}$$
$$|\dot{C}_L| \le \dot{C}_L^{\,max}$$
$$|\dddot{C}_L| \le \dddot{C}_L^{\,max}$$

and the terminal conditions

$$\mu(0) = \mu(t_f)$$
$$\gamma(0) = \gamma(t_f)$$
$$z(0) \le z$$
$$r(0) = r(t_f)$$
$$\theta(0) + \psi(0) = \theta(t_f) + \psi(t_f)$$

In words, we want to maximize the gain in velocity between the beginning and the end of the cycle. At the end of the cycle, the aircraft should have the same attitude with respect to the hurricane center, be at the same radius, and be at least at the same altitude as at the start of the cycle. Further, the aircraft starts at the bottom of the cycle, and begins to climb. Since μ and C_L are not governed by equations of motion, we added rate limits to guarantee smooth results. R_0 is a constraint set on the maximum radius of the aircraft. We adjusted this parameter to conduct the experiments in Section VI. In addition to the above constraints, we also place lower and upper bounds on V, ψ, γ, z, C_L, μ, S_w, m, and t_f.

As in [12], the formulation does not lend itself to an analytical solution, so we used a discrete approximation, where t_f was discretized as

$$t_f = \frac{k-1}{N-1} t_f, \quad k = 1, 2, ..., N$$

Let X be the vector of all optimization variables

$$X = [s_1, u_1, ..., s_N, u_N, S_w, m, t_f]^\top$$

s_k is a vector of state variables at time k, $s_k = [V_k, \psi_k, \gamma_k, x_k, y_k, z_k]^\top$; and u_k is a vector of control inputs at time k, $u_k = [C_{L,k}, \mu_k]^\top$. Since we neglect drag in our formulation, the aircraft design parameters were reduced to only the wing planform area (S_w) and aircraft mass (m) which were solved for as part of the optimization. Finally we also solved for t_f. Thus, in total X has dimension $8N + 3$.

The equations of motion, eqs. (8) to (10) and (15) to (17), were modeled as nonlinear equality constraints on X, and can collectively be referred to as

$$\dot{\mathbf{s}} = \mathbf{f}(\mathbf{s}, \mathbf{u})$$

As in [12], we approximate $\mathbf{x}$ as follows

$$\mathbf{s_{k+1}} = \mathbf{s_k} + \frac{\mathbf{t_{k+1}} - \mathbf{t_k}}{\mathbf{6}} (\mathbf{f_k} + \mathbf{4f_{m,k}} + \mathbf{f_k})$$

$$\mathbf{s_{m,k}} = \frac{1}{2} (\mathbf{s_{k+1}} + \mathbf{s_k}) + \frac{t_{k+1} - t_k}{8} (\mathbf{f_k} - \mathbf{f_{k+1}})$$

$$\mathbf{u_{m,k}} = \frac{1}{2} (\mathbf{u_{k+1}} + \mathbf{u_k})$$

where $\mathbf{f_{m,k}}$ is the midpoint value of $\mathbf{f}$ between t_k and t_{k+1}, which is found by inserting midpoint values of s and u into $\mathbf{f}$.

VI. Numerical Results for $n = 1, 2, 3$

For our numerical results, we also used Hurricane Charley as our archetype, with $W_{max} = 64$ m/s and $R_{max} = 11,000$ m being fixed for all simulations. For the wind field, we investigated exponents of $n = 1, 2, 3$, corresponding to wind velocity profiles that increased linearly, quadratically, and cubically with radius, respectively. The former was used to validate our analytical results from Section IV. Note all results reported in this section were found using a non-linear interior-point solver.

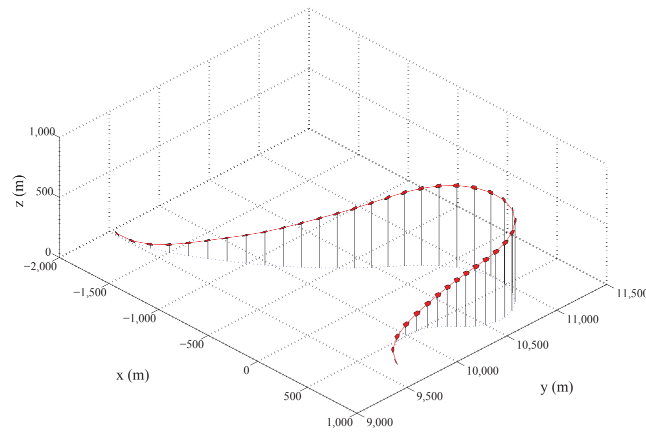

Fig. 2. Dynamic soaring trajectory at r=11,000 m for n=2. The hurricane windfield is blowing in the $-x$ direction in this plot. The aircraft climbs sharply against the wind, and then turns to dive with the wind, gaining veloicty. It ends the cycle at the same attitude as it started, but with an increase in airspeed of 4.57 m/s.

Figure 2 depicts a representative simulation result yielding a *feasible* dynamic soaring trajectory. In this instance, $n = 2$ and the trajectory was seeded at $r = 11,000$ m. The hurricane wind field is blowing in the $-x$ direction at this location. The aircraft begins the trajectory by climbing and turning into the wind field, losing airspeed. It then pitches down and dives with the wind field for the remainder of the cycle, gaining airspeed. At the end of the cycle the airspeed plot (Figure 3) indicates that the aircraft's airspeed increased by 4.57 m/s, while the altitude plot (Figure 4) indicates the aircraft ends the cycle at the same altitude as it started. Thus, the aircraft has a net gain in energy as it starts the next cycle – a successful dynamic soaring maneuver. Figures 3-4 also show the UAV airspeed and altitude vs. time for n=1 and n=3 under the same simulation conditions. Note that the airspeed gain for n=1 is 0 as expected, and for n=3 is higher than for n=2. We can attribute the latter result to the higher wind gradients for n=3 in the vicinity of the eyewall.

We hypothesized that energy gain was a function of the radius at which the UAV soars, and the

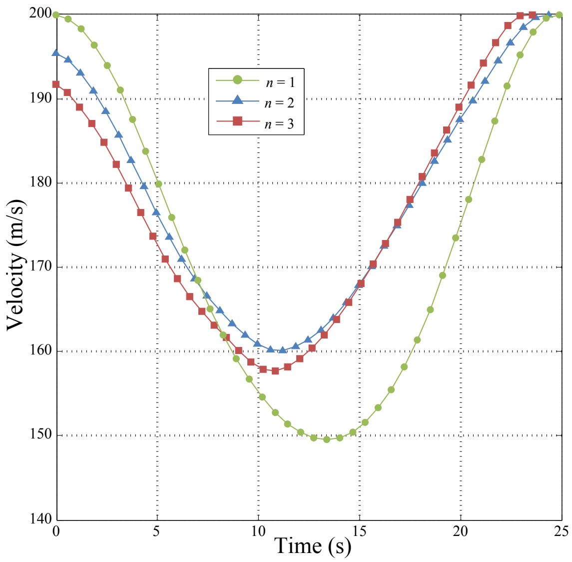

Fig. 3. Airspeed vs. time for a gliding UAV at r=11,000m for $n = 1, 2, 3$. For $n = 1$, there is no airspeed gain as expected. However, for $n = 2, 3$, higher final airspeeds are achieved through the dynamic soaring cycle. In all cases, V_{max} was constrained to 200m/s.

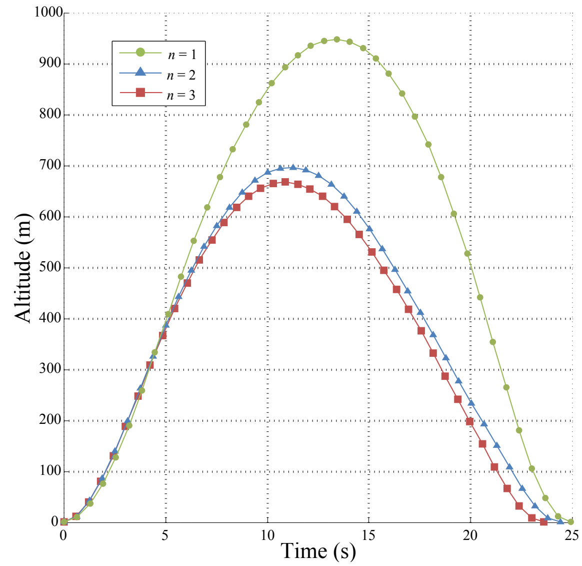

Fig. 4. UAV altitude vs. time for n=1,2,3. In each case, the aircraft starts at 0 altitude and ends the cycle at 0 altitude. Thus, for $n = 1$ energy remains neutral and for $n = 2, 3$ it has a net energy gain after one cycle.

wind field exponent of the hurricane. To test this, we conducted three sets of simulations - one for each hurricane exponent (n=1,2,3). In each set, we ran 11 trials with seed trajectories at radii from r=1,000 to r=11,000 meters, subject to the following additional constraint on the maximum radius

$$r \leq R_{max} - 1000j, \quad j = 0...10$$

In an attempt to reduce experiment variability, we fixed the aircraft parameters for all experiments to those recovered from the simulation shown in Figure 2. This converged to a solution with $S_w = 7.21$ m^2 and $m = 79.58$ kg. Results from these experiments are summarized in Figure 6, with the actual data shown as points and fitted linear/quadratic models shown by lines. For $n = 1$, at each radius the optimization returned a airspeed gain less than 10^{-6} m/s, which is effectively zero given our optimization tolerances. This was as expected given our findings in Section IV. For $n = 2$ or 3 however, there is an airspeed gain even at $r = 1000$ m. The data also suggested that the gain increases as a function of the radius. In an attempt to formalize this relationship, we examined the correlation between the empirically recovered airspeed gains ΔV and G defined as

$$G = \left[\left(\frac{\partial W_x}{\partial x}\right)^2 + \left(\frac{\partial W_x}{\partial y}\right)^2 + \left(\frac{\partial W_y}{\partial x}\right)^2 + \left(\frac{\partial W_y}{\partial y}\right)^2 \right]^{\frac{1}{2}}$$

which is an isotropic measure of the wind gradient. The resulting correlation coefficient for n=2,3 was very high ($\rho > 0.999$), indicating a linear relationship between the airspeed gain per cycle and the wind gradient. These results are summarized in Figure 5. Obtaining an analytical result to substantiate this hypothesis is currently ongoing.

VII. Discussion

In this paper, we investigated the potential for a gliding UAV to dynamically soar within a hurricane for long-term, in-situ storm monitoring. We provided both analytical and numerical results that indicate dynamic soaring may be possible for hurricanes with an acceptable wind profile, but physically impossible for others. In the former case, numerical results indicate a linear relationship between airspeed gain and wind field gradient. Obtaining an analytical result to support these findings is a topic of ongoing research.

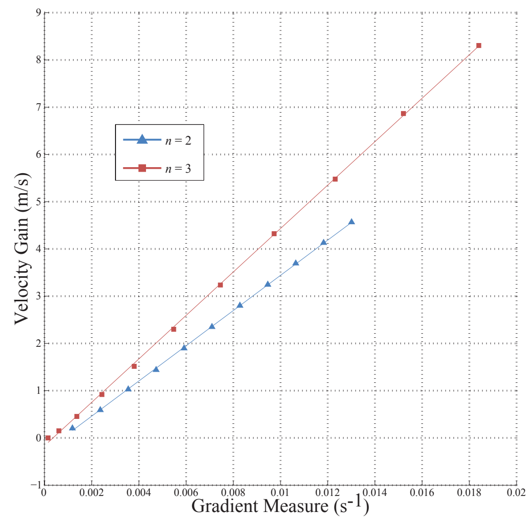

Fig. 5. Gradient measure G vs. cycle airspeed gain ΔV. Empirical results suggest a strong linear relationship between the two variables.

To date, our group's research in dynamic soaring aircraft has focused upon vertical wind gradients. We are currently manufacturing a carbon fiber UAV with a 6.5 meter wingspan capable of operating under very high load factors for dynamic soaring. Its potential for soaring in hurricanes will also be investigated.

ACKNOWLEDGMENTS

This material is based upon work supported by the National Science Foundation under Grant No. IIS-1065202. Any opinions, findings and conclusions or recommendations expressed in this material are those of the author(s) and do not necessarily reflect the views of the National Science Foundation (NSF).

REFERENCES

[1] J. Rayleigh, "The soaring of birds," *Nature*, vol. 27, pp. 534–535, 1883.

[2] C. D. Cone, "A mathematical analysis of the dynamic soaring flight of the albatross with ecological interpretations," Virginia Institute of Marine Science Special Scientific Report, Tech. Rep. 50, Oct. 1964.

[3] C. Sorrell. (2009, June) Dont blink: 392 mph glider tears through the air. Wired Magazine. [Online]. Available: http://www.wired.com/gadgetlab/2009/06/dont-blink-400mph-rc-gliders-tear-through-the-air/

[4] M. B. E. Boslough, "Autonomous dynamic soaring platform for distributed mobile sensor arrays," Sandia National Laboratories, Tech. Rep. SAND2002-1896, June 2002.

[5] Y. Zhao, "Optimal patterns of glider dynamic soaring," *Optimal Control Applications and Methods*, vol. 25, no. 2, pp. 67–89, 2004.

[6] G. Sachs and O. da Costa, "Periodic optimal control for dynamic soaring in the shear wind associated with jet streams," in *ICNPAA-2006: Mathematical Problems in Engineering and Aerospace Sciences*, Jun 2006.

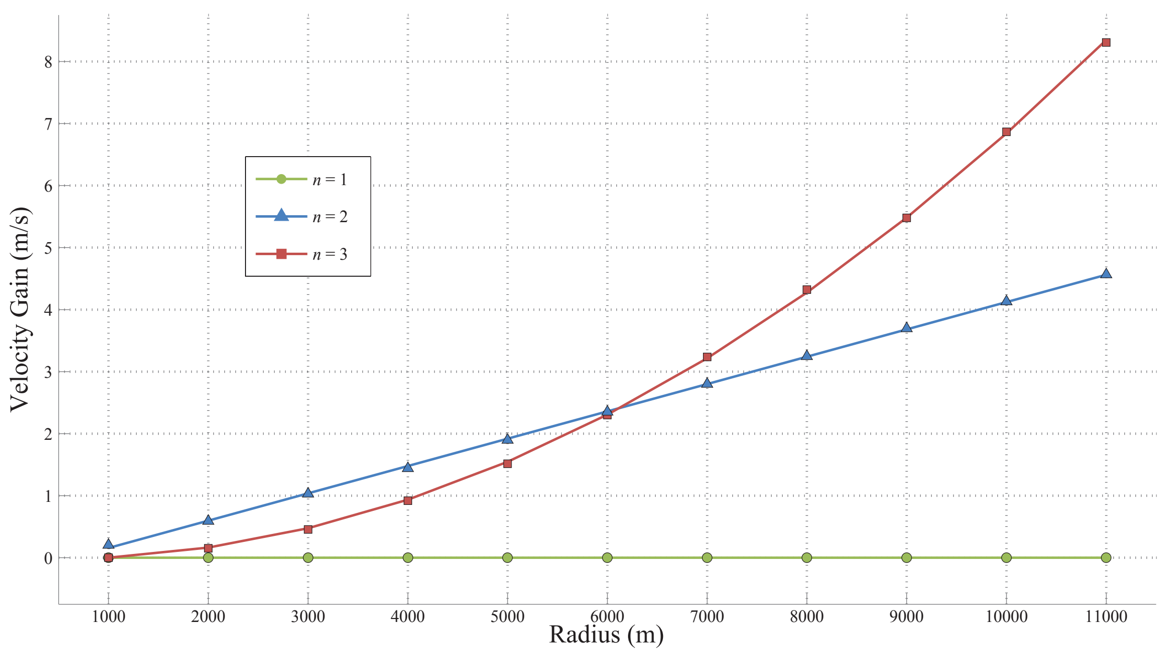

Fig. 6. Airspeed gain (ΔV) after one dynamic soaring cycle for three different wind field exponents at different radii. Data are indicated by shapes, while fitted models are indicated by lines. For $n = 1$ (green circles), no airspeed gain is possible; for $n = 2$ (blue triangles), airspeed gain increases linearly with radius; and for $n = 3$ (red squares), airspeed gain increases quadratically.

[7] R. J. Gordon, "Optimal dynamic soaring for full size sailplanes," Master's thesis, Air Force Institute of Technology, Wright-Patterson Air Force Base, Ohio, 2006.

[8] N. Akhtar, J. Whidborne, and A. Cooke, "Real-time trajectory generation technique for dynamic soaring uavs," in *Proc. International Conference on Control*, Manchester, U.K., Sep 2008.

[9] N. Lawrance and S. Sukkarieh, "Wind Energy Based Path Planning for a Small Gliding Unmanned Aerial Vechicle," in *AIAA Guidance, Navigation, and Control Conference*, Chicago, USA, August 2009.

[10] M. Deittert, A. Richards, C. Toomer, and A. Pipe, "Engineless Unmanned Aerial Vehicle Propulsion by Dynamic Soaring," *Journal of Guidance, Control, and Dynamics*, vol. 32, no. 5, pp. 1446–1457, Sep-Oct 2009.

[11] J. Grenestedt and J. Spletzer, "Optimal Energy Extraction During Dynamic Jet Stream Soaring," in *Proc. AIAA Guidance, Navigation and Control Conference*, Toronto, Ontario, Aug 2010.

[12] J. L. Grenestedt and J. R. Spletzer, "Towards Perpetual Flight of a Gliding Unmanned Aerial Vehicle in the Jet Stream," in *Proc. IEEE Conf. on Decision and Control (to appear)*, Atlanta, GA, Dec 2010.

[13] R. J. Pasch, E. S. Blake, H. D. Cobb, and D. P. Roberts, "Tropical cyclone report: Hurricane wilma," National Hurricane Center, Tech. Rep. TCR-AL252005, October 2005.

[14] M. A. Lander, "A tropical cyclone with a very large eye," *Monthly Weather Review*, vol. 127, pp. 137–142, 1999.

[15] C. Weatherford and W. M. Gray, "Typhoon structure as revealed by aircraft reconnaissance. part ii: Structural variability," *Monthly Weather Review*, vol. 116, pp. 1044–1056, 1988.

[16] T. Schott, C. Landsea, G. Hafele, J. Lorens, A. Taylor, H. Thurm, B. Ward, M. Willis, and W. Zaleski, "The saffir-simpson hurricane wind scale," National Weather Service, Tech. Rep., 2010. [Online]. Available: The Saffir-Simpson Hurricane Wind Scale

[17] H. E. Willoughby, R. W. R. Darling, and M. E. Rahn, "Parametric representation of the primary hurricane vortex. part ii: A new family of sectionally continuous profiles," *Monthly Weather Review*, vol. 134, pp. 1102–1120, Apr. 2006.

[18] R. J. Pasch, D. P. Brown, and E. S. Blake, "Tropical cyclone report: Hurricane charley," National Hurricane Center, Tech. Rep. TCR-AL032004, October 2004.